

1 **A core microbiota of the plant-earthworm interaction conserved across soils**

2

3 Samuel Jacquiod¹, Ruben Puga-Freitas², Aymé Spor¹, Arnaud Mounier¹, Cécile Monard³,

4 Christophe Mougel⁴, Laurent Philippot¹, Manuel Blouin^{1*#}

5

6 ¹Agroécologie, AgroSup Dijon, INRA, Univ. Bourgogne Franche-Comté, France

7 ²UMR 7618 IEES-Paris (CNRS, INRA, UPMC, IRD, UPEC), France

8 ³UMR 6553 ECOBIO (CNRS, Université de Rennes 1), France

9 ⁴UMR 1349 IGEPP (INRA - Agrocampus Ouest - Université Rennes 1), France

10 [#]Corresponding author: manuel.blouin@agrosupdijon.fr

11

12 **Abstract**

13 Microorganisms participate in most crucial soil functions and services benefiting human activities,
14 such as biogeochemical cycles, bioremediation and food production. Their activity happens
15 essentially in hotspots created by major soil macroorganisms, like rhizosphere and cast shaped by
16 plants and earthworms respectively¹. While effects of individual macroorganism on soil microbes
17 are documented, no studies attempted to decipher how the mosaic of microhabitats built by multiple
18 macroorganisms and their interaction determine the structure of microbial communities. Here we
19 show a joint shaping of soil bacterial communities by these two macroorganisms, with a prevalent
20 role of plants over earthworms. In a controlled microcosm experiment with three contrasted soils
21 and meticulous microhabitat sampling, we found that the simultaneous presence of barley and
22 endogeic earthworms resulted in non-additive effects on cast and rhizosphere bacterial
23 communities. Using a source-sink approach derived from the meta-community theory^{2,3}, we found
24 specific cast and rhizosphere *core microbiota*^{4,5} of the plant-earthworm interaction, detected in all
25 soils only when both macroorganisms are present. We also evidenced a *core network* of the plant-
26 earthworm interaction, with cosmopolitan OTUs correlated both in cast and rhizosphere of all soils.
27 Our study provides a new framework to explore aboveground-belowground interactions through the
28 prism of microbial communities. This multiple-macroorganisms shaping of bacterial communities
29 also affects fungi and archaea, while being strongly influenced by soil type. Further functional
30 investigations are needed to understand how these *core microbiota* and *core network* contribute to
31 the modulation of plant adaptive response to local abiotic and biotic conditions.

32

33 **Introduction**

34 While the structuring effect of plants on soil microbial communities is well-documented, the
35 overlooked role of earthworms on their abundance and activity may be as important^{6,7}, given that
36 they represent the highest animal biomass in soils⁸. Plants and earthworms are the major soil
37 ecosystem engineers⁹, shaping microhabitats¹⁰ populated with microbes originating either from
38 endogenic (e.g. endophytes and earthworm guts) or environmental (e.g. bulk soil) sources, namely
39 the rhizosphere and drilosphere (casts and burrows)¹. As such, plants and earthworms may be
40 regarded as competing biotic entities for the steering of soil microbial communities and functions.
41 Earthworms may even affect the assembly outcome of rhizosphere microbial communities¹¹, but the
42 reciprocal action of plant on drilosphere microbiota has never been investigated. Nevertheless,
43 positive interaction between these two macroorganisms is the rule, as earthworms increase plant
44 growth by ~25%^{12,13}. Furthermore, converging observations suggest that part of the mechanics
45 governing plant-earthworm relationships may pass through microbes^{14,15}. Therefore, they may also
46 be regarded as partners in shaping soil microbial communities.

47 Building on the concept of *core microbiota*^{4,5} associated with a host, we questioned the
48 existence of such an extended entity resulting from the interaction of multiple hosts by focusing on
49 plant and earthworm presence across soils. By looking at the right scale through the prism of
50 microhabitats (e.g. rhizosphere, cast and bulk), we expected to capture the reciprocal influences of
51 plant and earthworm on microbial communities, be they competitive, collaborative or neutral. We
52 looked at this interaction in three contrasted soils (clayed, loamy, sandy) using microcosms
53 containing either: i) a plant (barley, *Hordeum vulgare*), ii) endogeic earthworms (*Aporrectodea*
54 *caliginosa*), iii) both macroorganisms and iv) a control without macroorganism. After one month, we
55 applied a meticulous soil dismantling of each microcosm to separately harvest soil matrix (no
56 macroorganisms), rhizosphere, cast and their respective bulk soils (Supporting File 1). We focussed
57 on bacteria through 16S rRNA gene amplicon sequencing, because of their importance in the plant-

58 earthworm interaction¹⁶. We also monitored the total abundance of fungi, archaea and bacteria
59 using real-time quantitative PCR, as well as several plant traits.

60 **Results and discussion**

61 In accordance with the literature^{12,13}, we observed a positive effect of earthworms on shoot
62 biomass whatever the soil (+21%), associated with an increase in height (+5%) and leaf surface area
63 (+11%) in clayed and sandy soils (Tab.1). Beta-diversity analysis of bacterial community profiles
64 revealed a strong soil effect (Supporting File 2 and 3), calling for a refined analysis *by soil* (Fig.1).
65 Rhizosphere communities differed from those of other microhabitats, revealing the systematic plant
66 influence whatever the soil (CAP1, 18-24%) while earthworms effect was weaker and soil-
67 dependent (CAP2, 4-8%). Bulk and cast communities in earthworms treatment clustered away from
68 the control bulk matrix in the clayed soil, indicating an overruling earthworm effect (yellow apart
69 from blue, Fig.1a). However, earthworms had a weaker effect in the sandy soil, as bacterial
70 communities in bulk and cast were similar to the control (yellow close to blue, Fig.1c). The loamy
71 soil had an intermediate profile (Fig.1b).

72 The simultaneous presence of plant and earthworm resulted in non-neutral reciprocal effects
73 on bacterial communities. Earthworms influence on rhizosphere communities was always detected,
74 (CAP1-2, green and red triangles, Fig.1), with an average abundance increase of earthworm-
75 responding rhizosphere OTUs up to ~3-folds (Supporting File 4). Plant influence on cast
76 communities was also always detected, although weaker in the clayed soil (CAP2, yellow and red
77 squares, Fig.1), with an average abundance increase of plant-responding cast OTUs up to ~9-folds
78 in the sandy soil (Supporting File 4). As cast and rhizosphere community profiles with both
79 macroorganisms can not be predicted from the addition of their coordinates in single
80 macroorganisms treatments (Fig.1), our results demonstrated their significant interaction in shaping
81 microbial communities (Supporting File 3). Nevertheless, the strength of this interaction was
82 modulated by soil type, with a prevalent effect of plant in the sandy soil, and earthworms in the
83 clayed soil.

84 This plant-earthworm interaction questions the existence of a specific community sub-
85 sample amongst cast and rhizosphere bacteria, selected from *cosmopolitan OTUs present in all*
86 *soils*. Indeed, we detected a “*core microbiota*”^{4,5} of the earthworm/plant interaction *shared amongst*
87 *all soils*, featuring 106 OTUs (mostly Alphaproteobacteria and Actinobacteria), always observed in
88 casts and rhizospheres when both macroorganisms are present (purple and red intersect, Fig.2).
89 However, the presence of these ubiquitous OTUs is not necessarily specific to plant-earthworm
90 interaction *per se*. Therefore, we highlighted these community sub-samples using a “source-sink”
91 approach inspired from the metacommunity theory^{2,3} and based on parsimonious hierarchical
92 sorting¹⁷ to trace back probable origins of OTUs found in cast (g) and rhizosphere (h) microhabitats
93 when both macroorganisms were present (Fig.3a). We observed that the main source of bacteria
94 was the bulk matrix without any macroorganism (a: 72% in g; 65% in h), followed by the
95 microhabitats (bc, 13% in g; 20% in h) and other bulk soils (def, 6% in g; 4% in h). This “source-
96 sink” representation applied to all soils simultaneously revealed again a prevalent contribution of
97 plant (h: 18%, g: 6%) compared to earthworms (g: 7%, h: 2%), and evidenced endemic sub-samples
98 only seen in microhabitats whith both macroorganisms (g: 9%; h: 14%). We propose to call these
99 remaining cast and rhizosphere specific fractions emerging from their simultaneous presence in all
100 soils the “*core microbiota of the plant-earthworm interaction*”.

101 The plant-earthworm interaction may also be characterized *via* modifications of OTUs
102 abundance across soils regardless of their origins rather than species composition. We focused on
103 cosmopolitan OTUs found in all soils, and normalized their abundance variations relatively to their
104 control bulk matrix (z-score) in order to build correlation matrices for each microhabitat. We then
105 reconstructed a network specific of the plant-earthworm interaction by keeping only correlations
106 commonly found in cast and rhizosphere matrices, but absent in the bulk (see material and
107 methods). We found a cast and rhizosphere-specific network representing OTUs whose
108 standardized abundance was significantly modulated by plant-earthworm interaction (Fig.3b).
109 Similarly to the Venn diagram (Fig.2), this network was characterized by a phylogenetic signal in

110 favor of Actinobacteria and Alphaproteobacteria. The network was organized in three groups based
111 on hierarchical clustering of OTUs z-scores (Supporting File 5). These groups were in line with soil
112 types, indicating differentially altered abundance of these cosmopolitan OTUs when both
113 macroorganisms are present (barplot, Fig.3b). While other studies focused on identification of a
114 *core microbiota* specific to a given host^{4,5}, we expanded this concept to the interaction between
115 plant and earthworms *via* OTU correlations, evidencing a *core network* that enables the description
116 of multiple-macroorganisms shaping of bacterial communities.

117 Moreover, going beyond mere taxonomy, our qPCR results show that the outcome of this
118 interaction may affect other microbial domains. Indeed, the simultaneous presence of earthworms
119 and plants resulted in microbial abundance increase in microhabitats relative to their respective bulk
120 (z-score, Fig.4). This was observed in the loamy and sandy soils for bacteria, but also for fungi in
121 all soils, and archaea in the sandy soil (Fig.4, stars above lines), suggesting that their combined
122 presence have effects going beyond bacteria, impacting the whole microbial community. Moreover,
123 these increase in microbial abundances linked to macroorganism interaction were more frequent in
124 the sandy soil (two bacterial, one archaeal, one fungal, n = 4) compared to the loamy (one fungal, n
125 = 1) and clayed (n = 0) soils, suggesting stronger effects depending on soil type. Additionally, this
126 interaction was responsible in creation and/or reinforcement of so-called “hotspots”¹ relative to the
127 bulk soil (Fig.4, stars above bars). Likewise, hotspot numbers were soil-dependent, with higher
128 occurrence in the sandy soil (n = 6), compared to the loamy (n = 4) and clayed (n = 2) soils (Fig.4).

129 **Conclusion**

130 Altogether, our result indicated a joint shaping of bacterial communities by plant and
131 earthworm, correlating with an increase in plant biomass. This interaction resulted in the emergence
132 of i) *core microbiota* specific of plant-earthworm interaction revealed in cast and rhizosphere while
133 systematically present in all soils, as well as ii) a *core network* commonly shared between cast and
134 rhizosphere whose modularity was indicative of soil type. The contribution of the plant was always
135 dominant. Earthworms influence was soil-dependent, as well as plant-earthworm interaction, whose

136 importance was reinforced in the sandy soil. This joint shaping by two macroorganisms also
137 affected archaea and fungi, especially in the sandy soil. Our data suggest that the impact of the
138 interaction between these macroorganisms on microbial communities is more important when soil is
139 less fertile. Recent studies have accumulated evidences suggesting that microbial community
140 members may be recruited on a functional, rather than a taxonomic basis, also known as the “It is the
141 song, not the singers” theory¹⁸. Nevertheless, we show that the *core microbiota* resulting from
142 macroorganism interaction can be highlighted on a phylogenetic basis, with a taxa-specific
143 phylogenetic signal. A perspective based on an adaptive rationale would be to investigate these
144 multiple-macroorganisms *core microbiota* and *core network* on a functional basis¹⁹.

145 **Material and Methods**

146 *i. Microcosm establishment and sampling*

147 Three soils were used: a poor sandy soil classified as cambisol with moor (organic carbon: 14.7 g
148 kg⁻¹; total nitrogen: 1.19 g kg⁻¹; pH: 5.22; clay: 6.9%, loam: 19.0%, sand: 74.1%, origin: CEREEP,
149 Saint-Pierre-Lès-Nemours, France); a loamy crop soil classified as luvisol (organic carbon: 9.2 g
150 kg⁻¹; total nitrogen: 0.87 g kg⁻¹; pH : 7.0; clay: 16.7%, loam: 56.2%, sand: 27.1%, origin: INRA,
151 Versailles, France) and a forest clayed soil classified as leptosol (organic carbon: 56.7 g kg⁻¹; total
152 nitrogen: 4.65 g kg⁻¹; pH : 7.45; clay: 34.4%, loam: 39.2%, sand: 27.4%, origin: MNHN, Brunoy,
153 France). Only the first 20cm were sampled, excluding plant debris and roots. Soils were air-dried,
154 sieved (2mm) and set in microcosm pots of 1l containing 1kg of soil watered at 80% of their
155 respective water holding capacity, being the optimum for plant and earthworm²⁰. Four conditions
156 were tested with five biological replicates (Supporting File 1): i) plant alone, ii) three earthworms
157 alone, iii) both together and iv) nothing (control). Barley (commercial variety of *Hordeum vulgare*
158 L. from “La fermette”) was germinated in three batches of 80 seeds in Petri dishes containing each
159 soil moistened at 100% (20°C in phytotron, seven days), and ~8cm seedlings were transplanted in
160 pots. The earthworm species *Aporrectodea caliginosa* was chosen for its endogeic lifestyle.

161 Earthworms were coming from a non-stop breeding program started in 2007, with individuals
162 coming from the IRD park (Bondy, France). Three batches of young individuals were purged during
163 three days using their respective experimental soil to avoid massive contaminations from the
164 substrate used for breeding. Three individuals were introduced at the surface of pots, corresponding
165 to a total weight of ~1g. Microcosms were incubated in a climatic chamber (S10H, Conviron,
166 Canada) in the following conditions: 75% air humidity, 18/20°C night/day for a 12h photoperiod at
167 constant light intensity of 300 $\mu\text{mol photons m}^{-2} \text{ s}^{-1}$, for 28 days. Leaf surface was estimated after
168 17 days by summing leaf areas (one leaf area = leaf length x mid-section leaf width x 0.75; leaf-
169 specific correction coefficient for grass-like plants = 0.75)²¹. Plant height was estimated after 23
170 days based on the length of the longest leaf. Shoot biomass was measured after drying at 50°C for
171 48h. Soil was meticulously dismantled to sample distinct microhabitats: rhizospheric soil (thightly
172 adhering root soil at 70% humidity, recovered from vigorous shaking with distilled water, then
173 centrifuged), earthworm casts (visual identification)²² and bulk soil (remaining soil without visible
174 influence of roots and earthworms).

175 *ii. DNA extraction and qPCR settings*

176 Total microbial genomic DNA was extracted from 250 mg of soil, collected from the different
177 microhabitats, using FastDNA® SPIN Kit for Soil (MP Biomedicals) following manufacturer's
178 protocol. DNA concentration was quantified using Quant-iT™ dsDNA High-Sensitivity Assay Kit
179 (Invitrogen) before dilution at 1 ng. μl^{-1} . Abundances of fungal ITS (ITS3F: 5'-
180 GCATCGATGAAGAACGCAGC-3', ITS4R: 5'-TCCTCCGCTTATTGATATGC-3')²³,
181 Crenarchaeota 16S rRNA (Crenar771F: 5'-ACGGTGAGGGATGAAAGCT-3', Crenar975R: 5'-
182 CGGCGTTGACTCCAATTG-3')²⁴ and bacterial 16S rRNA genes (341F: 5'-
183 CCTACGGGAGGCAGCAG-3', 534R: 5'-CCTACGGGAGGCAGCAG-3')²⁵ in samples were
184 achieved using real-time polymerase chain reactions (qPCR) on a StepOnePlus™ Real-Time PCR
185 system (Applied Biosystem, France). The 15 μl reaction mixture was composed of 7.5 μl Power
186 SYBR™ Green PCR Master Mix with ROX (Applied Biosystem), 1.5 μl respective forward and

187 reverse primers (10 μ M), 2.5 μ l UltraPure™ DNase/RNase-Free Distilled Water (Applied
188 Biosystem) and 2 μ l DNA template. Potential qPCR reaction inhibition by DNA matrix was
189 assessed by doing a preliminary analysis adding 2 μ l of known concentration of plasmid to reaction
190 mixture previously described thus adjusting water volume to 0.5 μ l. No inhibition was detected as
191 amplification using primers targeting T7 and SP6 RNA polymerase promoters was similar among
192 samples. Conditions for real-time PCR were 900 s at 95 °C for enzyme activation followed by 35
193 cycles of 15 s at 95 °C, 30 s at specific annealing temperature (ITS/Archaea: 55°C, Bacteria: 60°C),
194 30 s at 72 °C for elongation and 30 s at 80 °C for data collection. Each abundance was quantified
195 with three repetitions using linearized plasmid-based standard curve with StepOne™ Software
196 v2.2.2. Deviation between the different qPCR plates was corrected using samples calibrator
197 presents in each plate. Amplicon copy numbers were normalized per μ gram of DNA per gram of
198 soil, transformed with log2, and used to build linear models. Normality of the data was assessed
199 with d'Agostino test on the residuals of each model (bacteria $p = 0.17$, fungi $p = 0.72$, archaea $p =$
200 0.36). Outlier values were removed based on ANOVA diagnosis plots. Respectively 3/96, 4/96 and
201 3/96 values were removed for bacteria, fungi and archaea respectively, leaving between 3-5
202 biological replicate values per condition. To account for the strong soil and macroorganism effects,
203 rhizosphere and cast datasets were standardized using their respective bulk soils under the
204 macroorganisms presence (z-score). Statistical significance against the bulk soil of the control
205 treatment and between microhabitats was tested with Student tests (one-sided, two-sample, $p <$
206 0.05). The one-sided version of the test was selected as we hypothesized that macroorganisms will
207 have a positive impact on molecular abundances of soil microorganisms.

208 *iii. 16S rRNA gene amplicon sequencing and bioinformatics*

209 Amplicons were generated from purified DNA in TE buffer by LGC Genomics (GmbH, Germany),
210 respecting the best practices guidelines^{26,27}. In the first step, the bacterial 16S rRNA gene V3-V4
211 hypervariable region was PCR-amplified using the fusion primers U341F (5'-
212 CCTACGGGNGGCWGCAG -3') and 785R (5'- GACTACHVGGGTATCTAAKCC -3')²⁸. For

213 each sample, the forward and reverse primers had the same 10-nt barcode sequence. PCR was
214 carried out in 20 μ L reactions containing containing 1.5 units MyTaq DNA polymerase (Bioline,
215 Germany) and 2 μ l of BioStabII PCR Enhancer (Sigma, Germany), 15pmol of each primer, and 5
216 ng template DNA. Thermal cycling conditions were 96°C for 2 min followed by 30 cycles of 96°C
217 for 15s, 50°C for 30sec and 70°C for 90s, with a final extension at 72°C for 10 min. PCR products
218 were visualized in 2% agarose gel to verify amplification and size of amplicons (around 500 bp).
219 About 20 ng amplicon DNA of each sample were pooled for up to 48 samples carrying different
220 barcodes, thus two pools of 48 samples were generated (n = 96). The amplicon pools were purified
221 using AMPure XP beads (Agencourt, Germany), followed by an additional purification on
222 MinElute columns (Qiagen, Germany). About 100 ng of each purified amplicon DNA pool was
223 used for Illumina library construction using the Ovation Rapid DR Multiplex System 1-96
224 (NuGEN, Germany). Illumina libraries were then pooled and size selected by preparative Gel
225 electrophoresis. Sequencing was performed on MiSeq (Illumina, 2x250 bp) using the MiSeq reagent
226 kit v2. Demultiplexing and trimming of Illumina adaptors and barcodes was done with Illumina
227 MiSeq Reporter software (version 2.5.1.3). Sequence data were analyzed using an in-house
228 developed Python notebook piping together different bioinformatics tools (available upon request).
229 Briefly, sequences were assembled using PEAR²⁹ with default settings, removing short sequences
230 and quality checks of the QIIME pipeline³⁰. Reference based and *de novo* chimera detection, as well
231 as clustering in OTUs were performed using VSEARCH³¹ and the Greengenes reference database.
232 The identity thresholds were set at 97%. Representative sequences for each OTU were aligned
233 using PyNAST³² and a 16S phylogenetic tree was constructed using FastTree³³. Taxonomy was
234 assigned using UCLUST³⁴ with the latest released Greengenes database³⁵, and the final contingency
235 table was set at OTU level. Rarefaction curves were calculated with the *vegan* package³⁶ in Rgui³⁷
236 to assess sequencing depth and samples were rarefied to 6900 counts.

237 *iv. Beta-diversity and multivariate analysis*

238 Rarefied OTU matrices and unifrac trees were used to build variance-adjusted weighted and
239 unweighted unifrac-based constrained analysis of principal coordinates (CAP, *capscale* function,
240 package *vegan*). Models were validated with 10,000 permutations. Responding OTUs whose
241 abundance was significantly altered in rhizosphere and casts when both macroorganisms were
242 present (but not in their respective bulk) were extracted using quasi-likelihood F-test under negative
243 binomial distributions and generalized linear models (nbGLM QLFT, FDR-adjusted $q < 0.05$).
244 OTUs significantly affected by the addition of a second macroorganisms in microhabitats were
245 extracted as previously described³⁸ via hierarchical clustering in heatmaps for cast (Supporting File
246 6) and rhizosphere samples (Supporting File 7), followed by grouping in barcharts (Supporting File
247 5).

248 v. *Venn diagram and source-sink plot*

249 A Venn diagram was done with the Rgui package *limma*³⁹ to define the core microbiota shared
250 between cast and rhizosphere using only cosmopolitan OTUs strictly found at least in 75% of
251 biological replicates (3/4) in all three soils (Figure 2). A “source-sink” plot was established to trace
252 OTU’s origin, using cosmopolitan OTUs found in 75% of biological replicates (3/4) in all three
253 soils. (Fig.2). We hypothesized that the sources of bacteria for casts (g) and rhizosphere (h)
254 communities in the presence of both macroorganisms were as follow: 1) the initial soil matrix
255 without macroorganisms (a); 2) the microhabitat created by each macroorganism alone (c for g and
256 e for h); 3) the second microhabitat created by the other macroorganism (e for g and c for h); 4) the
257 other microhabitat when both macroorganisms were present (h for g and g for h); 5) the bulk soil
258 surrounding the microhabitats from macroorganisms alone (b for g and d for h); 6) the bulk soil
259 surrounding the other microhabitats from macroorganisms alone (d for g and b for h); 7) the bulk
260 soil when both macroorganisms were present (f); 8) the remaining part was specifically attributed to
261 each microhabitat under interaction context as endemic fractions (g and h).

262 vi. *Core microbial network*

263 To account for the strong soil effect, OTU abundances in each sample were standardized to their
264 respective control bulk average and standard deviation without macroorganisms (z-score). We
265 focused on cosmopolitan OTUs present at least in 50% of samples in each soil ($n > 16/32$) and used
266 their standardized abundances to build three correlation networks, one per microhabitat, using
267 stringent cut-off (Spearman's $\rho < |0.6|$, FDR-adjusted $q < 0.05$). This resulted in a “bulk network”
268 (originating from all the standardized bulk samples in earthworm, plant, earthworm/plant treatments
269 in the three soils, $n = 36$), a “cast network” (originating from all the standardized cast samples in the
270 three soils, $n = 24$), and a “rhizosphere network” (originating from all the standardized rhizosphere
271 samples in the three soils, $n = 24$). Hereafter, we intersected the cast and rhizosphere networks to
272 only keep the overlapping correlations (exclusions and co-occurrences) in common between these
273 two microhabitats. Last, we removed any bulk interference correlations from the rhizosphere-cast
274 intersected network by subtracting correlations from the bulk network. This network arithmetic was
275 done with the Rgui package *igraph*⁴⁰. Modularity in the network was attributed based on
276 hierarchical clustering of their standardized abundances (Supporting File 5), which was summarized
277 in the upper-right barplot of Fig.3, classifying OTUs in three modules based on their average z-
278 score behavior across the three soils.

279 **Acknowledgements**

280 We thank Valérie Serve for technical help, Beatriz Decencière, Amandine Hansart and Florent
281 Massol of the CEREEP - Ecotron IDF/UMS CNRS/ENS 3194 for the sandy soil, Sandrine Salmon
282 of the UMR 7179 / CNRS-MNHN for the clayed soil and Christophe Montagnier of the UE
283 Grandes cultures / INRA for the loamy soil. This work was supported by grants from the French
284 national program CNRS/INSU [EC2CO-Biohefect-MicrobiEn-AuxAzote].

285 **Author contributions and information**

286 SJ (analytical strategy, data analysis, manuscript writing), RPF (laboratory experiment, manuscript
287 editing), CMon (sequencing strategy), CMou (sequencing strategy), AS (analytical strategy, data

288 analysis, manuscript editing), AM (bioinformatic), LP (analytical strategy, manuscript editing), MB
289 (study conception, research direction, analytical strategy, manuscript writing). Authors declare no
290 competing interests.
291

292 **Code and data availability**

293 The Rgui software and associated function packages used for data analysis are all publically
294 available. Data that support the findings of this study have been deposited in the Sequence Read
295 Archive database (SRA, <https://www.ncbi.nlm.nih.gov/sra>) with the primary accession code
296 “SUB5123378”, and will be made automatically publically available after publication.

297 **References**

- 298 1. Kuzyakov, Y., Blagodatskaya, E. Microbial hotspots and hot moments in soil: Concept &
299 review. *Soil Biol Biochem* **83**, 184e199 (2015).
- 300 2. Mouquet, N., Loreau, M. Community patterns in source-sink metacommunities. *Am Nat*
301 **162**, 544-557 (2003).
- 302 3. Lindegren, M., Andersen, K.H., Casini, M., Neuenfeldt, S. A metacommunity perspective
303 on source-sink dynamics and management: the Baltic Sea as a case study. *Ecol Appl* **24**,
304 1820-1832 (2014).
- 305 4. Lundberg, D.S. *et al.* Defining the core *Arabidopsis thaliana* root microbiome. *Nature* **488**,
306 86-90 (2012).
- 307 5. Turnbaugh, P.J. *et al.* A core gut microbiome in obese and lean twins. *Nature* **457**, 480-484
308 (2009).
- 309 6. de Menezes, A.B. *et al.* Earthworm-induced shifts in microbial diversity in soils with rare
310 versus established invasive earthworm populations. *FEMS Microbiol Ecol* **94**, doi:
311 10.1093/femsec/fiy051 (2018).
- 312 7. Fjøsne, T.F., Stenseth, E.B., Myromslien, F., Rudi, K. Gene expression of TLR homologues
313 identified by genome-wide screening of the earthworm *Dendrobaena veneta*. *Innate Immun*
314 **21**, 161-166 (2018).
- 315 8. Bouché, M.B. Lombriciens de France. Ecologie et Systématique. Institut national de la
316 recherche agronomique. *Annls zool-ecol animale* **72**, 1-671 (1972).
- 317 9. Jones, C.G., Lawton, J.H., Shachak, M. Organisms as Ecosystem Engineers. *Oikos* **69**, 373-
318 386 (1994).
- 319 10. Lavelle, P. *et al.* Soil function in a changing world: the role of invertebrate ecosystem
320 engineers. *Eur J Soil Biol* **33**,159-193 (1997).
- 321 11. Braga, L.P. *et al.* Disentangling the influence of earthworms in sugarcane rhizosphere. *Sci*
322 *Rep* **6**, 38923 (2016).

- 323 12. van Groenigen, J.W. *et al.* Earthworms increase plant production: a meta-analysis. *Sci Rep*
324 **4**, 6365 (2014).
- 325 13. van Groenigen, J.W. *et al.* How fertile are earthworm casts? A meta-analysis. *Geoderma*
326 **338**, 525-535 (2018).
- 327 14. Puga-Freitas, R., Barot, S., Taconnat, L., Renou, J.P., Blouin, M. *et al.* Signal molecules
328 mediate the impact of the earthworm *Aporrectodea caliginosa* on growth, development and
329 defence of the plant *Arabidopsis thaliana*. *PLoS One* **7**, e49504 (2012).
- 330 15. Blouin, M. Chemical communication: An evidence for co-evolution between plants and soil
331 organisms. *Appl Soil Ecol* **123**, 409-415 (2017).
- 332 16. Hoeffner, K., Monard, C., Santonja, M., Cluzeau, D. Feeding behaviour of epi-aneic
333 earthworm species and their impacts on soil microbial communities. *Soil Biol Biochem* **125**,
334 1-9 (2018).
- 335 17. MacArthur, R.H., Wilson, E.O. *The Theory of Island Biogeography*. Princeton, NJ:
336 Princeton University Press, 1967. 203 p. ISBN 978-0-691-08836-5.
- 337 18. Doolittle, W.F., Inkpen, S.A. Processes and patterns of interaction as units of selection: An
338 introduction to ITSNTS thinking. *Proc Natl Acad Sci U S A* **115**, 4006-4014 (2018).
- 339 19. Lemanceau, P., Blouin, M., Muller, D., Moëgne-Loccoz, Y. Let the Core Microbiota Be
340 Functional. *Trends Plant Sci* **22**, 583-595 (2017).
- 341 20. Lavelle, P. Les vers de terre de la savane de Lamto (Côte d'Ivoire). Peuplements,
342 populations et fonctions de l'écosystème. *Publ lab Zool ENS* **12**, 1301 (1978).
- 343 21. Blouin, M., Lavelle, P., Laffray, D. Drought stress in rice (*Oryza sativa* L.) is enhanced in
344 the presence of the compacting earthworm *Millsonia anomala*. *Env Exp Bot* **60**, 352-359
345 (2007).
- 346 22. Velasquez, E. *et al.* This ped is my ped: Visual separation and near infrared spectra allow
347 determination of the origins of soil macroaggregates. *Pedobiologia* **51**, 75-87 (2007).
- 348 23. White, T.J. Amplification and Direct Sequencing of Fungal Ribosomal RNA Genes for
349 Phylogenetics. *PCR Protocols, a Guide to Methods and Applications*. Biochemical
350 Education **19**, 315-322. Edited by Innis, M.A., Gelfand, D.H., Sninsky, J.J, White T.J. 482
351 p. Academic Press, London 1990. ISBN 0-12-372181-4.
- 352 24. Ochsenreiter, T., Selezi, D., Quaiser, A., Bonch-Osmolovskaya, L., Schleper, C. Diversity
353 and abundance of Crenarchaeota in terrestrial habitats studied by 16S RNA surveys and real
354 time PCR. *Environ Microbiol* **5**, 787-797 (2003).
- 355 25. Muyzer, G., de Waal, E.C., Uitterlinden, A.G. Profiling of complex microbial populations
356 by denaturing gradient gel electrophoresis analysis of polymerase chain reaction-amplified
357 genes coding for 16S rRNA. *Appl Environ Microbiol* **59**, 695-700 (1993).

- 358 26. Berry, D., Mahfoudh, K.B., Wagner, M., Loy, A. Barcoded Primers Used in Multiplex
359 Amplicon Pyrosequencing Bias Amplification. *Appl Environ Microbiol* **77**, 7846-7849.
360 (2011).
- 361 27. Schöler, A., Jacquiod, S., Vestergaard, G., Schulz, S., Schloter, M. Analysis of soil
362 microbial communities based on amplicon sequencing of marker genes. *Biol Fertil Soils* **53**,
363 485 (2017).
- 364 28. Klindworth, A. *et al.* Evaluation of general 16S ribosomal RNA gene PCR primers for
365 classical and next-generation sequencing-based diversity studies. *Nucleic Acids Res* **41**, e1
366 (2013).
- 367 29. Zhang, J., Kobert, K., Flouri, T., Stamatakis, A. PEAR: a fast and accurate Illumina Paired-
368 End reAd mergeR. *Bioinformatics* **30**, 614-620 (2014).
- 369 30. Caporaso, J.G. *et al.* (2010). QIIME allows analysis of high-throughput community
370 sequencing data. *Nat Methods* **7**, 335-336.
- 371 31. Rognes, T., Flouri, T., Nichols, B., Quince, C., Mahé, F. VSEARCH: a versatile open source
372 tool for metagenomics. *PeerJ* **4**, e2584 (2016).
- 373 32. Caporaso, J.G. *et al.* Global patterns of 16S rRNA diversity at a depth of millions of
374 sequences per sample. *Proc Natl Acad Sci U S A* **108**:4516-4522 (2011).
- 375 33. Price, M.N., Dehal, P.S., Arkin, A.P. FastTree: computing large minimum evolution trees
376 with profiles instead of a distance matrix. *Mol Biol Evol* **26**, 1641-1650 (2009).
- 377 34. Edgar, R.C. Search and clustering orders of magnitude faster than BLAST. *Bioinformatics*
378 **26**, 2460-2461 (2010).
- 379 35. McDonald, D. *et al.* An improved Greengenes taxonomy with explicit ranks for ecological
380 and evolutionary analyses of bacteria and archaea. *ISME J* **6**:610-608 (2012).
- 381 36. Dixon, P. VEGAN, a package of R functions for community ecology. *J Veg Sci* **14**, doi:
382 10.1111/j.1654-1103.2003.tb02228.x (2009).
- 383 37. R Development Core Team. R. A language and environment for statistical computing. R
384 Foundation for Statistical Computing. Vienna: RC Team; 2017. <http://www.R-project.org>
385 (2017).
- 386 38. Jacquiod, S. *et al.* Long-term soil metal exposure impaired temporal variation in microbial
387 metatranscriptomes and enriched active phages. *Microbiome* **6**, 223 (2018).
- 388 39. Ritchie, M.E. *et al.* limma powers differential expression analyses for RNA-sequencing and
389 microarray studies. *Nucleic Acids Res* **43**, e47 (2015).
- 390 40. Csardi, G., Nepusz, T. The igraph software package for complex network research.
391 *InterJournal Complex Systems* **1695**. <http://igraph.org> (2006).
- 392

394 **Legends for figures and tables:**

395 **Tab.1:** Effect of earthworms presence on barley traits at harvest in each soil. Three traits were
396 measured (rows), including height (the longest leaf length, which was always the highest in our
397 case), dry shoot weight and leaf surface area. Statistical significance was tested using two-sided,
398 two-sample Student tests ($p < 0.05$) to compare average values (\pm standard error of the mean)
399 between the condition without (w/o ew) and with (w ew) earthworms. Lowercase letters indicate
400 statistically significant difference between tested average values (“a”: highest, “b”: lowest). All
401 tested conditions were set with five biological replicates ($n = 60$).

402 **Fig.1:** Canonical analysis of principal coordinates of bacterial communities in each soil (CAP,
403 variance adjusted weighted unfrac distances). CAP1 and 2 represent the constrained components
404 with their respective percentage of the total variance explained. Each model was validated using
405 10.000 permutations. The four treatments are indicated by different colors, while microhabitats are
406 indicated by different marker shapes (Total $n = 96$).

407 **Fig.2:** Venn diagram and taxonomy of the core microbiota shared between casts and rhizosphere
408 when both macroorganisms are present (in white, $n = 106$). Only OTUs found at least in 75% of the
409 biological replicates (3/4) and in all three soils were considered. The piechart shows the unweighted
410 taxonomic distribution of the 106 OTUs, mainly dominated by Actinobacteria ($n = 60$) and
411 Alphaproteobacteria ($n = 24$) ($n = 48$ samples).

412 **Fig.3: Panel a.** Source-sink plot tracing the origin of OTUs coming from “sources” (a-f) going into
413 “sinks” (here the cast and rhizosphere when both macroorganisms are present, g and h). Only OTUs
414 found in 75% of biological replicates (3/4) and in the three soils were included ($n = 465$).
415 Hierarchical sorting was applied to attribute OTU source from the following orders respectively for
416 the cast sink “g”: {abchdef} and the rhizosphere sink “h”: {acbgedf}. Source contributions are
417 indicated in percentages, with discontinuous light-grey arrows for contributions $< 3\%$, and no
418 arrows if contribution was null ($n = 96$). **Panel b.** Core network of OTUs found in cast and

419 rhizosphere of all soils. Module membership (node shapes) was attributed based on OTU
 420 standardized abundances against control bulk matrices as shown in the upper-right barchart
 421 (average z-score \pm standard error of the mean, $n = 48$). When both macroorganisms were present,
 422 diamond-shaped OTUs abundance increased in sandy soil, but decreased in clayed soil. Conversely,
 423 circle-shaped OTUs abundance decreased in sandy soils while increasing in clayed soils. Triangle-
 424 shaped OTUs increased in all soils, especially in the loamy soil.

425 **Fig.4:** qPCR estimation of bacterial/archaeal genetic markers (a and b, 16S rRNA gene) and fungi
 426 (c, ITS). Molecular copy counts were standardized against average and standard deviation values of
 427 reference bulk soils from the same treatment (z-score). Barcharts are representing z-score averages
 428 \pm standard error of the mean ($n = 3-5$). Significance between treatments were all assessed by two-
 429 sample, one-sided Student tests. Significance: *** $p < 0.001$; ** $p < 0.01$; * $p < 0.05$; . $p > 0.1$.

430 **Figures and Table**

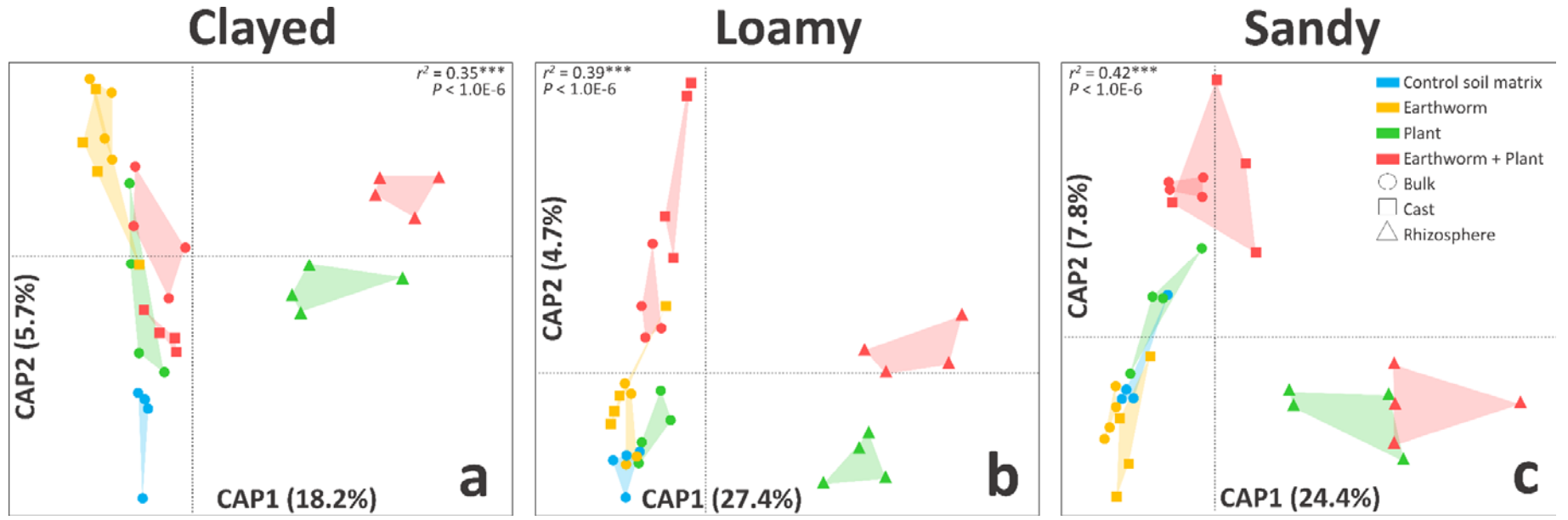
431 **Table 1**

Soil	clayed		loamy		sandy	
	-	+	-	+	-	+
Earthworms						
Height (mm)	34.80 \pm 0.26 ^b	37.10 \pm 0.80 ^a	30.30 \pm 0.51	31.10 \pm 0.60	32.10 \pm 0.56 ^b	34.30 \pm 0.44 ^a
Dry shoot weight (g)	0.44 \pm 0.01 ^b	0.60 \pm 0.05 ^a	0.32 \pm 0.03 ^b	0.37 \pm 0.03 ^a	0.36 \pm 0.01 ^b	0.44 \pm 0.02 ^a
Surface (mm²)	47.59 \pm 2.88 ^b	54.20 \pm 2.51 ^a	36.22 \pm 2.32	35.50 \pm 2.26	41.63 \pm 1.83 ^b	47.33 \pm 2.49 ^a

432

433

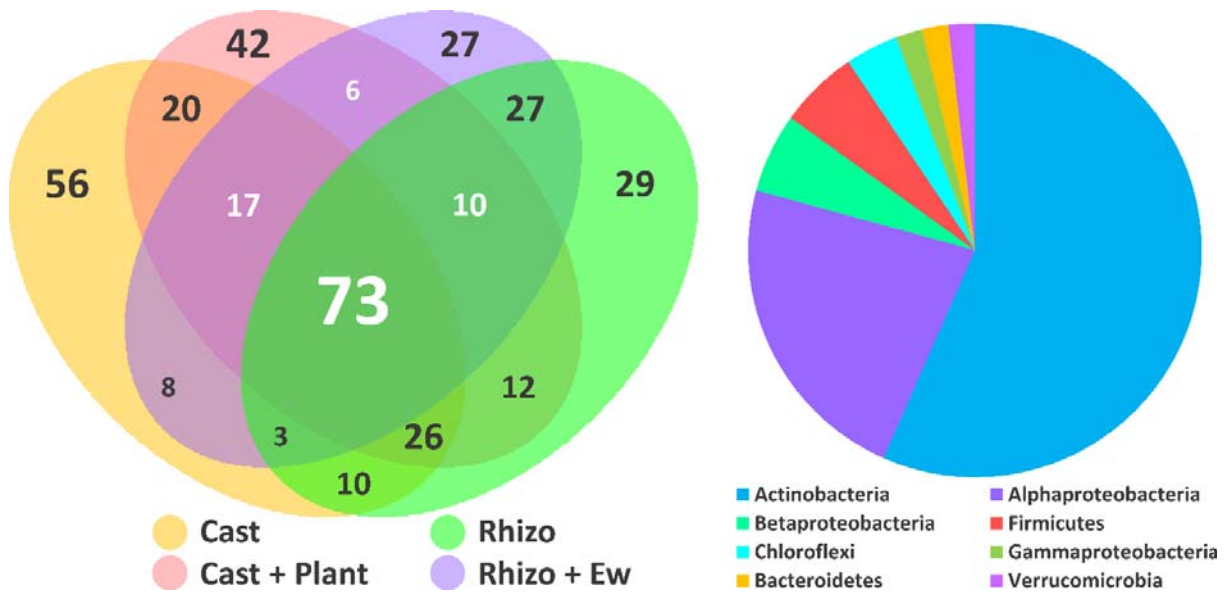
434 **Figure 1**



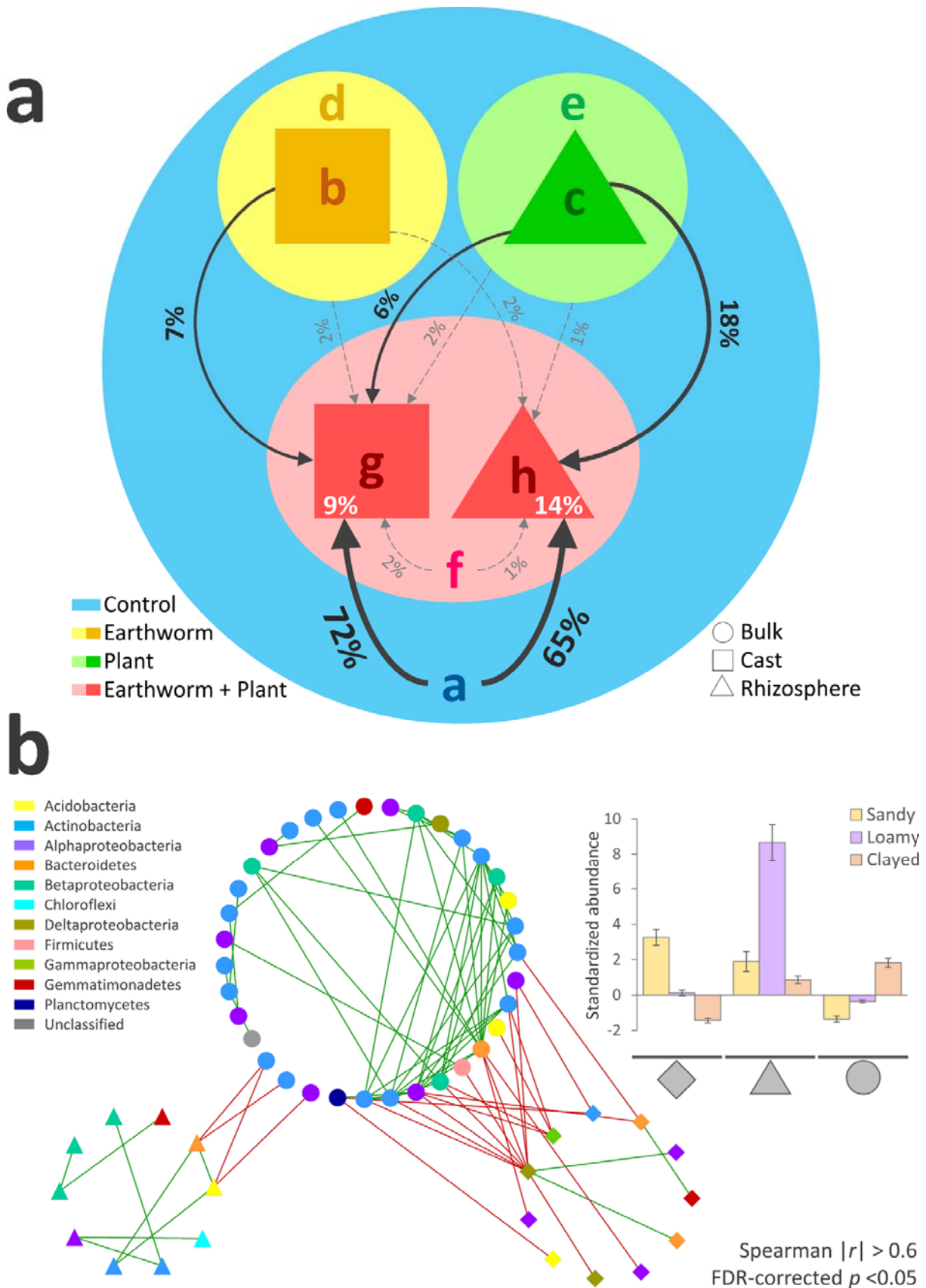
435

436

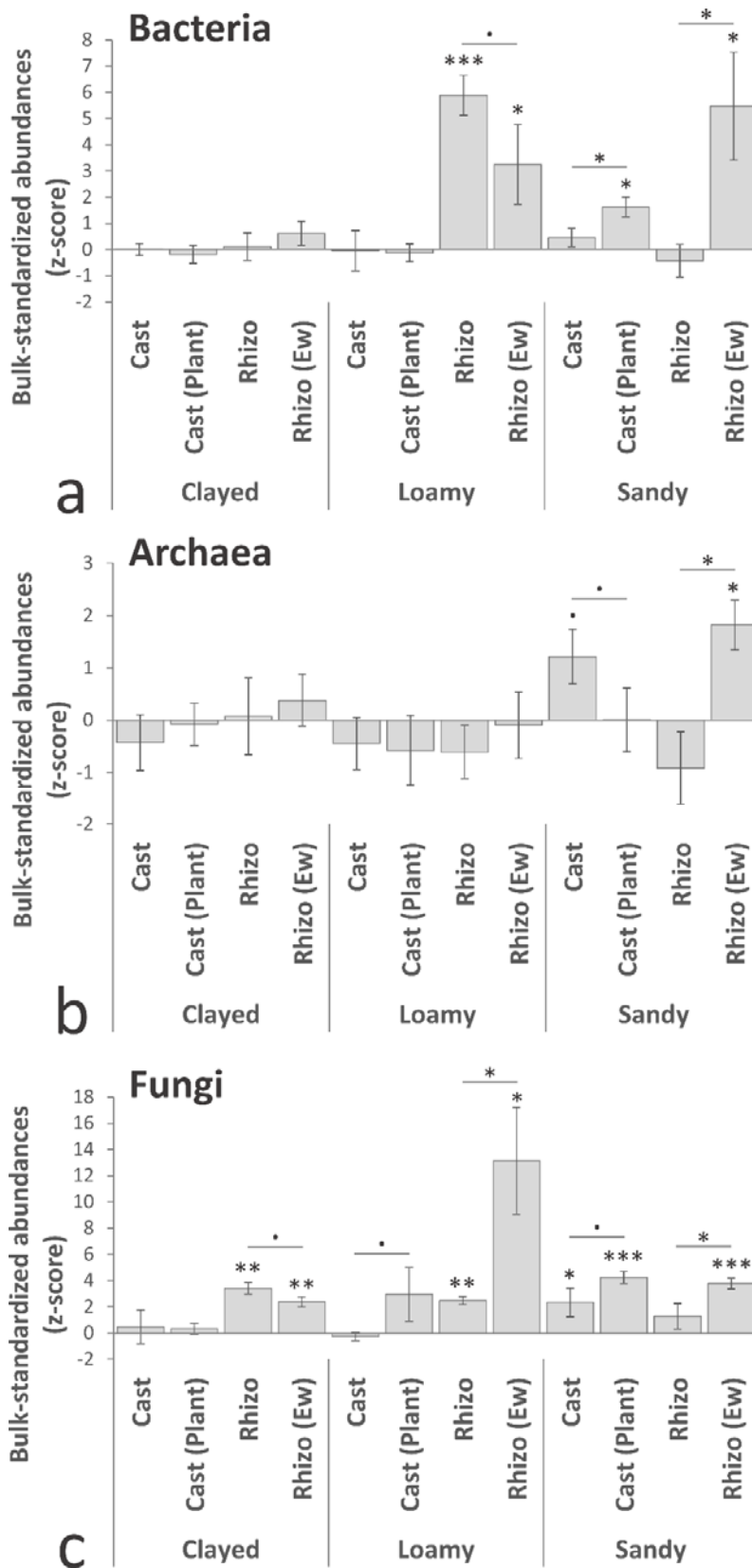
437 **Figure 2**



440 **Figure 3**



442 **Figure 4**



443